Strong Two-Mode Parametric Interaction and Amplification in a Nanomechanical Resonator

Sungwan Cho,[1,2,3] Sung Un Cho,[3] Myunglae Jo,[3,‡] Junho Suh,[1] Hee Chul Park,[4] Sang Goon Kim,[1,5] Seung-Bo Shim,[1,*] and Yun Daniel Park[3,†]

[1]*Korea Research Institute of Standards and Science, Daejeon 34113, Republic of Korea*
[2]*Graduate School of Nanoscience and Technology, Korea Advanced Institute of Science and Technology, Daejeon 34141, Republic of Korea*
[3]*Department of Physics and Astronomy, Seoul National University, Seoul 08826, Republic of Korea*
[4]*Center for Theoretical Physics of Complex Systems, Institute of Basic Science, Daejeon 34051, Republic of Korea*
[5]*Department of Physics, Chungnam National University, Daejeon 34134, Republic of Korea*

(Received 5 December 2017; revised manuscript received 31 March 2018; published 14 June 2018)

We demonstrate a scheme for amplifying nanomechanical motion based on strong parametric interactions between two independent flexural modes of a *single* nanobeam. A static electric field polarizes a dielectric nanobeam and additional radio-frequency voltage excites the motion of the beam. When the excitation frequency equals the difference of the two resonance frequencies, we observe a mode-splitting feature in the strong-coupling regime. If the excitation frequency overlaps the sum of the two resonance frequencies, the optical signal from the thermal motion of the nanomechanical resonator is amplified by more than 30 dB. We demonstrate that coupling between the odd- and even-numbered oscillatory mode can be realized and a coupled-mode theory is developed from a simple capacitor model to explain our observations. We conclude that the results are thoroughly explained by parametric interactions between two independent nanomechanical modes in thermal motion. This observation of parametric control can be employed in nanomechanical force detection and molecular sensing applications.

DOI: 10.1103/PhysRevApplied.9.064023

I. INTRODUCTION

Nanomechanical systems have attracted research interest from diverse scientific and engineering fields as they exhibit unique characteristics such as versatile coupling to different physical systems [1–5], high sensitivity to external forces [6], compatibility with conventional electronics and semiconductor processes [7], and low-power operation [8]. Recently, these potentials have been realized in ultrasensitive mass spectroscopy [9,10], quantum-limited force measurements [11,12], and coherent quantum converters [13,14]. While many of these applications require ever smaller and lighter mechanical devices to improve performance, the size of the mechanical system is often incommensurate with the efficiency of the electronic or optical transduction of nanomechanical motion: the coupling between the mechanical resonator and the motion transducer generally diminishes as the system size is reduced.

To address this issue, a direct amplification of mechanical motion is pursued with efforts to identify a low-noise amplification method universally applicable to various sensing applications. Degenerate parametric amplification in a nanomechanical cantilever was reported [15], with subsequent studies of parametric amplification in nanomechanical devices demonstrating its applicability to harmonic force detection [16,17] and resonator motion control, such as through quadrature squeezing [18,19]. However, degenerate parametric amplification is fundamentally phase sensitive and requires phase information of the weak signal under study, which is difficult to acquire *a priori*.

Further, it has been shown that two resonant oscillators coupled by a time-varying nonlinear component can become a nondegenerate parametric amplifier in both electrical and optical domains [20,21]. In the mechanical domain, application of the sum frequency of different resonant modes has shown an enhancement of resonantly driven mechanical motions in a torsional structure [22,23]. Despite these possibilities of developing a mechanical nondegenerate amplifier, the detailed mechanism based on their structure and flexural motion is not fully understood.

Our work presents an idea to apply the nondegenerate mechanical amplification technique to a single

*Corresponding author.
seungbo2@kriss.re.kr
†Corresponding author.
parkyd@phya.snu.ac.kr
‡Present address: Nanoelectronics Group, Service de Physique de l'Etat Condensé, CEA Saclay, F-91191 Gif-sur-Yvette, France.

nanomechanical structure with multiple resonant modes. The technique utilizes coupling between different flexural modes in mechanical resonators via the mechanical motion itself [24–30]; more specifically, our method is based on the dielectric gradient force transduction scheme [31]. By modulating the electric field acting on a dielectric nanobeam (or pump) at the difference between the resonance frequencies of two independent modes, we observe parametric coupling between two nanomechanical modes in thermal motion. When the pump frequency reaches the sum of the two resonance frequencies, an amplification of thermomechanical motion occurs [32]. At stronger pump amplitude, we observe nondegenerate parametric amplification of thermal motion at two pump frequencies different from the exact sum frequency of the two flexural modes, following a decrease in amplification gain at the exact pump frequency. We provide a theoretical treatment from general Euler-Bernoulli equations that explains these complex dynamics thoroughly, suggesting that this coupling and amplification process arises from nondegenerate parametric interactions between two normal modes in the single nanomechanical oscillator. Furthermore, our observation presents that the coupling between flexural modes is very sensitive and becomes possible without additional structure for asymmetry [33] between flexural modes of different parity. A numerical analysis based on experimental parameters is also provided to support our theoretical model.

II. DESIGN AND EXPERIMENT

We fabricate an 80-μm-long, doubly clamped nanobeam from a 200-nm-thick silicon nitride thin film with high tensile stress (>700 MPa) [Fig. 1(a)]. Side electrodes are in the vicinity of the resonator with 200-nm vertical gaps [inset of Fig. 1(a)] to maximize the dipole interaction between the electric field and mechanical structure. A dc voltage between the side electrodes induces a dipole moment on the mechanical resonator, and a rf voltage actuates the mechanical motion of the nanobeam by dipole interaction between the resonator and modulated electric field, which is known as the dielectric gradient force [31].

The device is maintained at high vacuum (approximately 7.5×10^{-4} Pa) to minimize viscous damping effects on the nanomechanical motion and at room temperature

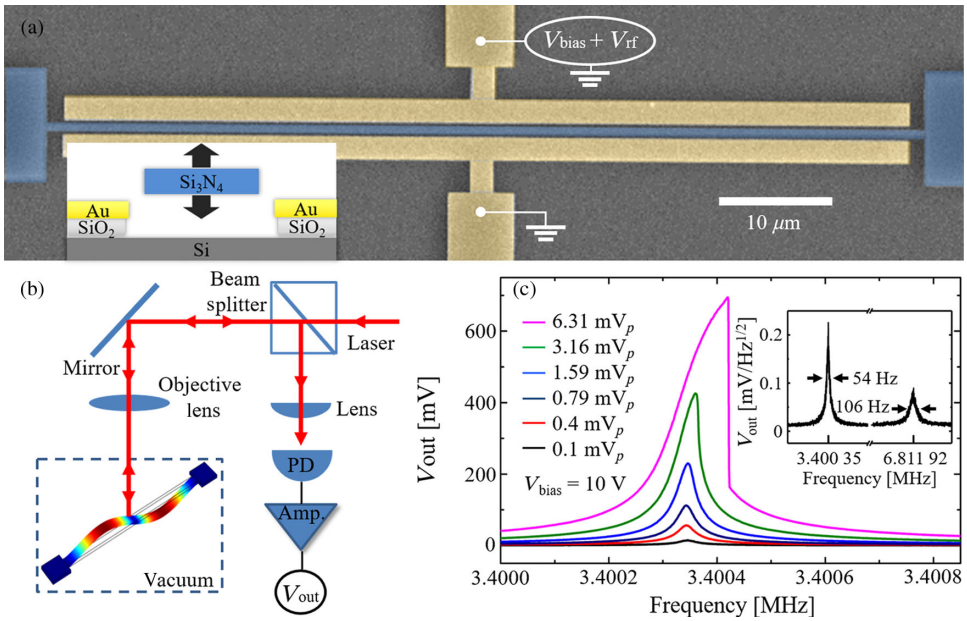

FIG. 1. Description of the nanoelectromechanical resonator and optical measurement scheme. (a) Scanning electron micrograph of the nanomechanical beam resonator and side electrodes with false color. The doubly clamped beam (blue) is in thermal motion, and a rf signal (resonant or parametric pump) in combination with dc bias is applied via metal electrodes (yellow). The parametric pump is tuned to the frequency of the difference (red detuned) or the sum (blue detuned) of the frequency of its first and second flexural modes. The inset depicts a schematic diagram of the cross-sectional geometry of the nanomechanical device. (b) Schematic diagram of the optical measurement based on amplitude modulation from the surface of the nanomechanical structure. An intensity-stabilized He-Ne laser beam is directed to the mechanical resonator through a beam splitter and mirror and tightly focused on the surface of the device by an objective lens. The reflected beam is focused onto the photodetector (PD) by a plano-convex lens. The amplitude-modulated signal is recorded by the PD, and spectral information is analyzed by a spectrum analyzer (SA) or a network analyzer (NA). (c) Driven and thermal motion of the nanomechanical resonator. With a strong resonant-driving signal (V_{rf}) near its resonant frequency, the nanomechanical resonator presents a clear nonlinear response. The inset shows the fundamental and second flexural modes of the resonator in thermal motion without V_{rf}. Driven response is detected by the NA, and the response of thermal motion to parametric pump is investigated using the SA.

$(293.0 \pm 0.1$ K) while reducing temperature fluctuation during measurement. The spectral responses of motion are monitored using optical reflectance measurements to transduce the nanomechanical motion [Fig. 1(b)] [34]. This measurement scheme provides sufficient sensitivity to observe multiple flexural modes in thermal motion.

We first characterize the driven and thermomechanical motion of the nanomechanical resonator. The addition of a rf voltage (pump) on the side electrodes actuates the nanomechanical oscillator through the dielectric gradient force. In a trivial regime, where the frequency ω_p of the applied rf voltage $V_{\rm rf}$ is close to ω_1 or ω_2, we detect resonant excitation of these modes and a nonlinear response [Fig. 1(c)]. We also observe the thermomechanical motion of fundamental ($f_1 = \omega_1/2\pi \approx 3.400\,35$ MHz) and second ($f_2 = \omega_2/2\pi \approx 6.811\,92$ MHz) flexural modes with only dc voltage applied on the side electrodes. These modes possess low dissipation rates ($\Gamma_1 = \omega_1/Q_1 \approx 2\pi \times 54$ Hz, $\Gamma_2 = \omega_2/Q_2 \approx 2\pi \times 106$ Hz) with a high-frequency-Q product over $fQ = 4.3 \times 10^{11}$ Hz for the second mode [35,36], as shown in the inset of Fig. 1(c). High-frequency flexural motion and a high mechanical quality factor come from the high tensile stress in the silicon nitride layer [36]. Furthermore, the frequency of the resonant modes becomes close to an integer multiple of the resonant frequency of the fundamental mode [37,38], which is usually observed in string-type mechanical resonators.

More interesting responses are revealed in the nonresonant regime, when ω_p equals the difference ($\omega_{\rm red} = \omega_2 - \omega_1 = 2\pi \times 3.411\,57$ MHz) or the sum ($\omega_{\rm blue} = \omega_2 + \omega_1 = 2\pi \times 10.212\,27$ MHz) of the two resonance frequencies. Since the force generated by the pump is off resonant to both flexural modes in this case, the leading-order effect of the pump on the mechanical oscillators is to modulate their effective spring constant ("parametric excitation"). Furthermore, ω_p is also different from either $2\omega_1$ or $2\omega_2$, and, thus, a nondegenerate parametric process should dictate the mechanical motion of the two modes.

III. THEORETICAL MODEL

To analyze the nondegenerate parametric dynamics of two flexural modes sharing the same nanomechanical beam structure in our experiment, we include a simple capacitor model with a dielectric that oscillates at its natural frequency by thermal energy between the two side electrodes. The electrostatic energy of the capacitor structure (nanoelectromechanical resonator and two side electrodes) can be described as $U(u;t) = \frac{1}{2}C(u)V(t)^2$, where $C(u)$ is the capacitance of the device including mode shape and displacement of the nanomechanical resonator, with $u(z,t) = \sum_n \phi_n(z)\chi_n(t)$ at longitudinal position z and time t, and $V(t)$ is the time-varying applied voltage between the side electrodes at pump frequency ω_p. The total capacitance of the device is approximated as $C_{\rm total} \cong \int_0^l \{[\varepsilon_o w\sqrt{1+u'(z)^2}]/[d+u(z)]\}dz$, where $u'(z) = \{[\partial u(z)]/(\partial z)\}$ is the curved geometry along the longitudinal axis by the flexural mode shape of thermal motion, and l is the length of the nanomechanical resonator (for a detailed description of this model, see the Supplemental Material [39]). This curvature creates higher-order terms in forces on the nanomechanical resonator, and the linearized presentation of force to the normal direction is as follows:

$$F_c(u,u';t) \approx -C_0\left[\int_0^l dz \sum_{mn} \phi_m(\phi_n/d^2 + \phi_n'')\chi_n\right] \times (V_{\rm bias}^2 + 2V_{\rm bias}V_{\rm rf}\cos\omega_p t). \quad (1)$$

Different flexural modes are coupled to each other by the geometry of the nanomechanical resonator. The dielectric gradient force is included by $V_{\rm bias}$ and $V_{\rm rf}$; in the absence of rf voltage $V_{\rm rf}$, the force on the nanomechanical resonator is quadratically proportional to $V_{\rm bias}$, with resonant frequency also tuned quadratically. This resonant frequency tuning of each flexural mode by applied bias voltage is shown in the inset of Fig. 2(n).

Then, the governing equation for a doubly clamped beam driven via dipole force is

$$\rho A\frac{\partial^2 u}{\partial t^2} + EI_y\frac{\partial^4 u}{\partial z^4} + \Gamma\frac{\partial u}{\partial t} - p_0\frac{\partial^2 u}{\partial z^2} - f_c(u,u';t) = 0. \quad (2)$$

Here, there is time-dependent coupling between the different modes caused by the oscillation of capacitive force with parametric pump frequency ω_p. To investigate the spectral response of the nanomechanical resonator with this time-dependent coupling between different flexural modes, we transform the governing equation for a doubly clamped nanomechanical resonator in Euler-Bernoulli form with coupling force [Eq. (2)] into a generalized coupled equation as follows:

$$\ddot{\chi}_m + \gamma_m\dot{\chi}_m + \omega_{m0}^2\chi_m + \sum_{n=1,2} k_{mn}(V_{\rm bias}^2 + 2V_{\rm bias}V_{\rm rf}\cos\omega_p t)\chi_n = 2F_d\cos\omega_d t, \quad (3)$$

which includes the driving force to describe the driven oscillation by thermal energy. For the interaction between the two flexural modes, we can simplify Eq. (3) into a coupled-mode equation of two modes [40–43]. A detailed derivation of theoretical model can be found in the Supplemental Material [39],

$$\ddot{\chi}_1 + \gamma_1\dot{\chi}_1 + \omega_1^2(V_{\text{bias}})\chi_1 + 2\cos(\omega_P t)\sum_{n=1,2}\kappa_{1n}\chi_n = 2F_d\cos(\omega_d t), \quad (4)$$

$$\ddot{\chi}_2 + \gamma_2\dot{\chi}_2 + \omega_2^2(V_{\text{bias}})\chi_2 + 2\cos(\omega_P t)\sum_{n=1,2}\kappa_{2n}\chi_n = 2F_d\cos(\omega_d t). \quad (5)$$

For the coupled equation of motion, κ_{mn} represents the parametric $(m = n)$ and coupling $(m \neq n)$ coefficient including the structural asymmetry between the flexural modes of a beam. As the nanomechanical resonator is in thermal motion, we include $F_d\cos(\omega_d t)$ for the thermal driving force, with the amplitude of F_d affecting only the relative amplitude of the spectral response of the nanomechanical resonator. Here, γ_i and $\omega_i(V_{\text{bias}})$ are the damping rate and resonant frequency of the ith flexural mode modified by dc bias voltage.

To compare with experimental results, we evaluate nondegenerate parametric coupling and amplification using slowly varying amplitude solutions by solving the coupled equations (4) and (5) for the first and second flexural modes.

IV. DISCUSSION

To confirm the parametric coupling between flexural modes in thermal motion, we apply a parametric pump near the red-detuned sideband frequency $(\omega_p \sim \omega_{\text{red}})$ and

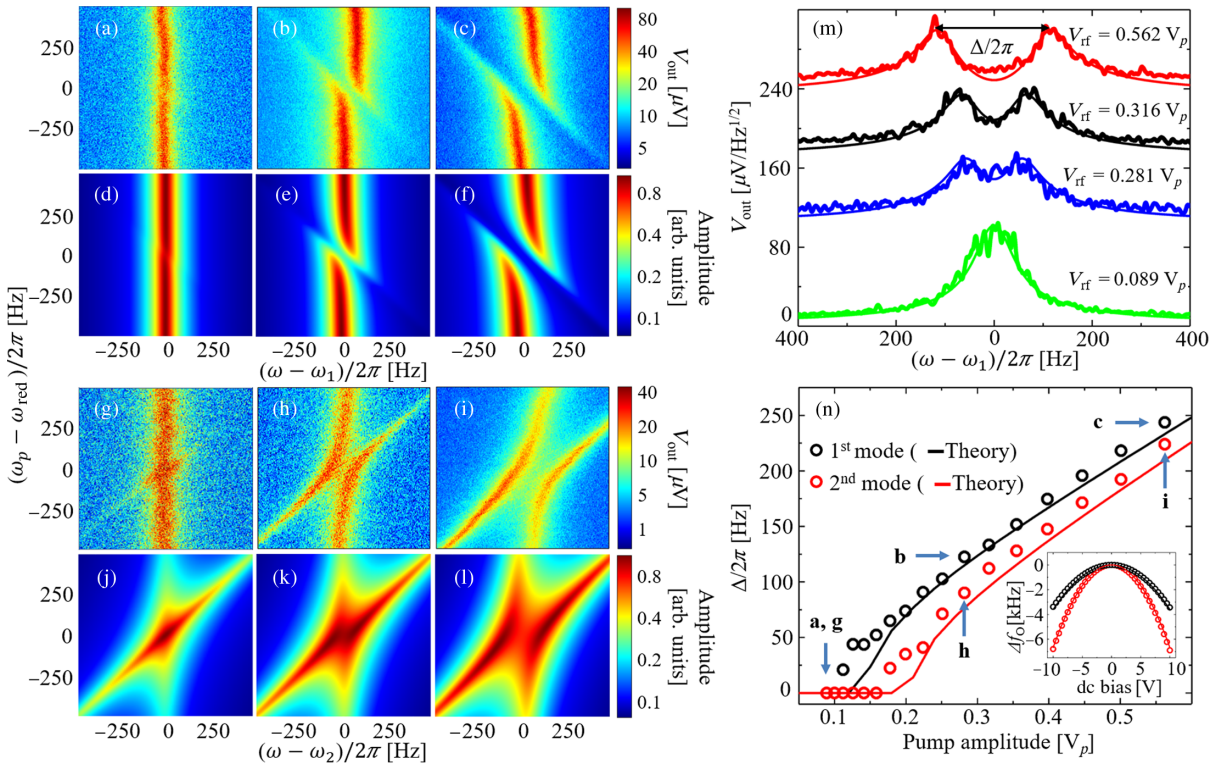

FIG. 2. Parametric coupling by red-detuned sideband pump. (a)–(c),(g)–(i) Parametric coupling between the first and second flexural modes, respectively. Responses of the first and second modes of the nanomechanical resonator to a parametric pump near the red-detuned sideband frequency $\omega_{\text{red}} = \omega_2 - \omega_1$ for different pump amplitudes: $V_{\text{rf}} = 0.089$ V [(a),(g)], 0.316 V [(b),(h)], and 0.562 V [(c),(i)]. Spectral response of each flexural mode is recorded by a SA while sweeping pump frequency ω_P from $\omega_{\text{red}} - 500 \times 2\pi$ to $\omega_{\text{red}} + 500 \times 2\pi$. At $V_{\text{rf}} = 0.089$ V, there is no apparent normal mode splitting for either flexural mode when $\omega_p = \omega_{\text{red}}$. At $V_{\text{rf}} = 0.316$ V, the mode-splitting frequency is estimated to be 135 and 115 Hz and increases to 245 and 223 Hz with $V_{\text{rf}} = 0.562$ V for the first and second modes, respectively. (d)–(f),(j)–(l) Numerical analysis for the responses of the first and second flexural modes, respectively, derived from slowly varying ω amplitudes of Eqs. (2) and (3) for frequency of interest near mechanical resonant frequency, and $\omega_p \sim \omega_{\text{red}}$, the parametric pump frequency with different pump amplitudes (see the Supplemental Material [39]). (m) Spectral response of the first flexural mode in thermal motion to different parametric pump amplitudes and the theoretically estimated spectrum of flexural modes. Each spectrum is offset for clarity on the same scale. At $V_{\text{rf}} = 0.089$ V$_p$, the amplitude of the resonant spectrum of the nanomechanical resonator decreases, and the dissipation rate increases to 134 Hz without normal mode splitting. At larger parametric pump amplitudes, the normal-mode-splitting feature becomes more explicit. (n) Mode-splitting frequency by applied parametric pump amplitude from $V_{\text{rf}} = 0.089$ to 0.562 V$_p$ for both flexural modes. The theoretically estimated mode-splitting frequency is shown as a solid line for each mode. The inset demonstrates the capacitive tuning of resonant frequency by applied dc bias voltage df/dV approximately -350 and -700 Hz/V for the first and second flexural modes at 10-V dc.

observe the spectral response of the nanomechanical resonator. With the lowest peak amplitude of applied parametric pump ($V_{\rm rf} = 0.089$ V$_p$), the resonant peak of the first mode is broadened ($\Gamma_1 \approx 2\pi \times 140$) and deamplified [Fig. 2(a)]. This broadening effect is also observable in the second mode [Fig. 2(g)]; however, the spectral amplitude of the second mode does not decrease. This amplitude disparity by the red-detuned sideband pump is attributed to an energy transfer from the first to second mode by mode coupling [24].

The mode-splitting feature becomes noticeable at stronger pump amplitudes, as shown in Figs. 2(b) and 2(c) for the first mode and Figs. 2(h) and 2(i) for the second mode. Mode-splitting enhancement and deamplification of the first mode by different pump amplitudes at exact red-detuned sideband parametric pump frequency ($\omega_p = \omega_{\rm red}$) is shown in Fig. 2(m). The mode-splitting feature has an onset at finite pump amplitudes for both first and second modes; we note that the onset of normal-mode splitting at finite parametric pump amplitudes is also observed in cavity optomechanical systems, which couple microwave and optical cavities to mechanical resonators with dissipation [5,44]. For our system with parametric coupling between flexural modes, we can observe a different onset of pump amplitude due to the larger dissipation rate of the second mode. With different pump amplitudes, we extract the mode-splitting frequency by extracting the peak separation from two peaks at $\omega_p = \omega_{\rm red}$. The measured frequency splitting shows an onset at a pump amplitude of 0.28 V$_p$ and increases linearly up to approximately 230 Hz (first mode) and 220 Hz (second mode) by the applied parametric pump [Fig. 2(n)]. This clear normal-mode-splitting feature

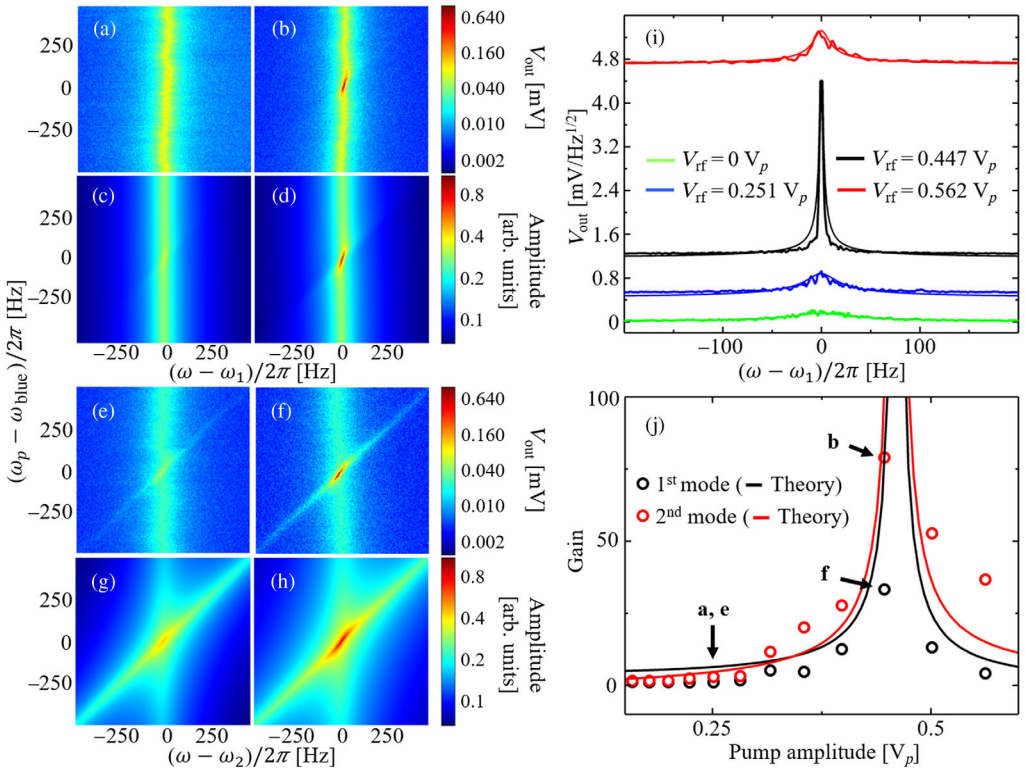

FIG. 3. Nondegenerate parametric amplification by blue-detuned sideband pump. (a),(b) Spectral responses of nondegenerate parametric amplification of the first flexural mode with different pump amplitude of $V_{\rm rf} = 0.251$ and 0.447 V$_p$, correspondingly. (c),(d) Numerical calculation of nondegenerate parametric amplification in the first flexural mode with the same pump amplitude as experiment. (e),(f) Nondegenerate parametric amplification of the second flexural modes with the same pump amplitudes used for the first mode. (g),(h) Numerically attained color maps of the spectral response of the second mode. The frequency of parametric pump ω_P is swept from $\omega_{\rm blue} - 500 \times 2\pi$ to $\omega_{\rm blue} + 500 \times 2\pi$Hz for $V_{\rm rf} = 0.251$ to 0.447 V$_p$. At $V_{\rm rf} = 0.251$ V$_p$, the amplification of thermal motion by parametric pump is not clear and gain is close to unity. However, the amplification gain reaches its maximum when $V_{\rm rf}$ is increased to 0.447 V$_p$ for both first and second flexural modes. (i) Nondegenerate parametric amplification of the resonant spectrum of the first flexural mode by the blue-detuned parametric pump. Each spectrum is offset to display the displacement of the mechanical structure at the same scale. The resonant spectrum for $V_{\rm rf} = 0.562$ V$_p$ (red) corresponds to $\omega_P \sim \omega_{\rm blue} + 25 \times 2\pi$ to consider frequency drift during the measurement process. (j) Real gain of nondegenerate parametric amplification by the parametric pump at the exact blue-detuned sideband frequency $\omega_P = \omega_{\rm blue} = \omega_2 + \omega_1$. Real gain is calculated by the ratio of the peak amplitudes with the parametric pump to the peak amplitude without the parametric pump. Maximum gain is approximately 33 and 79 for the first and second modes, respectively. The theoretically expected gain to the applied parametric pump is shown as a solid line.

and small dissipation rate ($\Delta > \Gamma_1, \Gamma_2$) demonstrate that this system is in the strong-coupling regime by the parametric sideband pump.

We now extend the mode-coupling physics to the nondegenerate parametric process in order to amplify the motion of the nanomechanical resonator. Vibrational motion in both flexural modes is amplified with the parametric pump at the blue-detuned sideband ($\omega_{\text{blue}} = \omega_2 + \omega_1$). In contrast to phase-sensitive, degenerate parametric amplification, here there is no phase relation between the pump and each flexural mode (ω_p, ω_1, ω_2); therefore, nondegenerate parametric interaction can be beneficial to detect or exploit unexpected signals without preliminary information of their phase correlation.

With a blue-detuned parametric pump on a thermally driven mechanical structure in experiment, we can expect the nondegenerate parametric amplification effect for both flexural modes. With a small parametric pump amplitude of 0.251 V_p, the amplification gain of the optical signal is close to unity for both the first and second modes. With a higher pump amplitude of 0.447 V_p, nondegenerate parametric amplification presents its maximum gain of 33 (approximately 30 dB) and 79 (approximately 38 dB) for the first and second modes, respectively. We attain a color map of the spectral response of the nanomechanical resonator to the parametric pump with different pump amplitude and frequency by numerically solving the slowly varying amplitude solution of Eqs. (4) and (5). These color maps present that the amplification phenomena are also generated at the same pump amplitude as shown in Figs. 3(c) and 3(d) and Figs. 3(g) and 3(h). The resonant spectrum of the first mode with increasing pump amplitude by blue-detuned sideband pump ($\omega_p = \omega_{\text{blue}}$) is shown in Fig. 3(i) with the theoretically estimated resonant spectrum. A theoretical analysis based on our model shows good agreement with the experimentally acquired gain for both flexural modes. The gain can be approximated as $G \sim \{A/[1 - (\kappa^2)/(\gamma_1\gamma_2\omega_1\omega_2)]\}^2$, where $\kappa = \kappa_{12} = \kappa_{21}$ is the coupling constant in Eqs. (4) and (5), γ_i and ω_i are the dissipation rate and resonant frequency of each mode, respectively, and A is a constant (see the Supplemental Material [39]). In the regime where the coupling constant κ becomes close to the product of the dissipation rate and resonant frequency $\sqrt{\gamma_1\gamma_2\omega_1\omega_2}$, the gain increases and approaches its maximum value. However, for $\kappa > \gamma_1\gamma_2\omega_1\omega_2$, where the parametric pump power is stronger than that of the maximum amplification gain, the amplification gain decreases, and the experimental results align well with theoretical estimation. The estimated parametric pump amplitude for maximum gain also coincides with the experimental result, as seen in Fig. 3(j). The discrepancy in gain between theory and experiment is presumably attributed to the small temperature fluctuation during the measurement and nonlinear damping [45,46], which are not considered in our theoretical model. Although the amplification gain at exact blue-detuned sideband frequency decreases for a higher amplitude of parametric pump over 0.447 V_p, we can observe a peak-splitting feature at different pump frequency, which needs more detailed study (see the Supplemental Material [39]).

V. CONCLUSION

In conclusion, we demonstrate parametric mode interaction in the strong-coupling regime between two flexural modes of a nanomechanical resonator by modulating the external electric field. With a parametric pump at the red-detuned sideband of the first and second modes, both mechanical modes present a clear normal-mode-splitting feature, with a splitting frequency over 230 Hz. Using the same technique with a blue-detuned sideband pump, we realize nondegenerate parametric amplification of thermal motion, with the amplification gain reaching 33 (approximately 30 dB) and 79 (approximately 38 dB) in amplitude for the first and second modes, respectively. The nanomechanical resonator also exhibits resonant spectrum splitting by strong parametric pumping. These results demonstrate that parametric dynamics between normal modes can be achieved by modulating external parameters rather than strain-mediated coupling by resonant driving. With potential for active nonlinear devices [47,48] and mechanical logic devices [49,50], coupling based on an external control parameter as shown here can be extended to multiple mechanical modes of distinct devices and coupled hybrid systems. Moreover, nondegenerate parametric amplification can be suitable for various sensing applications considering its advantages in amplifying the motional amplitude of the device as well as high gain in the absence of preliminary phase information.

ACKNOWLEDGMENTS

S. C. acknowledges support from the Basic Science Research Program through the National Research Foundation of Korea (NRF) funded by the Ministry of Science, ICT and Future Planning (Grant No. NRF-2017R1C1B1012047) and the BK21 PLUS program of Graduate School of Nanoscience and Technology, KAIST through the NRF funded by the Ministry of Education. J. S. acknowledges support from the Basic Science Research Program through the NRF funded by the Ministry of Science, ICT and Future Planning (Grants No. NRF-2016R1C1B2014713 and No. NRF-2016R1A5A1008184) and from the Korea Research Institute of Standards and Science project "Convergent Science and Technology for Measurements at the Nanoscale." H. C. P. acknowledges support from Center for Theoretical Physics of Complex Systems, Institute of Basic Science (Grant No. IBS-R024-D1).

S. C. and S. U. C. designed the experiment, and S. C. and M. J. designed and fabricated the doubly clamped

nanomechanical devices. S. C., S. G. K., and S. B. S. designed and performed detailed optical measurements. J. S. and H. C. P. analyzed the experimental result and provided the theoretical modeling and calculation with S. B. S. and S. C. Y. D. P. and S. B. S. managed the experimental process with theoretical analysis. All authors helped in the manuscript preparation.

[1] G. Zolfagharkhani, A. Gaidarzhy, P. Degiovanni, S. Kettemann, P. Fulde, and P. Mohanty, Nanomechanical detection of itinerant electron spin flip, Nat. Nanotechnol. **3**, 720 (2008).

[2] O. Arcizet, V. Jacques, A. Siria, P. Poncharal, P. Vincent, and S. Seidelin, A single nitrogen-vacancy defect coupled to a nanomechanical oscillator, Nat. Phys. **7**, 879 (2011).

[3] S. Camerer, M. Korppi, A. Jöckel, D. Hunger, T. W. Hänsch, and P. Treutlein, Realization of an Optomechanical Interface between Ultracold Atoms and a Membrane, Phys. Rev. Lett. **107**, 223001 (2011).

[4] G. A. Steele, A. K. Hüttel, B. Witkamp, M. Poot, H. B. Meerwaldt, L. P. Kouwenhoven, and H. S. J. van der Zant, Strong coupling between single-electron tunneling and nanomechanical motion, Science **325**, 1103 (2009).

[5] S. Gröblacher, K. Hammerer, M. R. Vanner, and M. Aspelmeyer, Observation of strong coupling between a micromechanical resonator and an optical cavity field, Nature (London) **460**, 724 (2009).

[6] J. Moser, J. Güttinger, A. Eichler, M. J. Esplandiu, D. E. Liu, M. I. Dykman, and A. Bachtold, Ultrasensitive force detection with a nanotube mechanical resonator, Nat. Nanotechnol. **8**, 493 (2013).

[7] J. L. Lopez, J. Verd, J. Teva, G. Murillo, J. Giner, F. Torres, A. Uranga, G. Abadal, and N. Barniol, Integration of RF-MEMS resonators on submicrometric commercial CMOS technologies, J. Micromech. Microeng. **19**, 015002 (2009).

[8] J. Arcamone, B. Misischi, F. Serra-Graells, M. A. F. van den Boogaart, J. Brugger, F. Torres, G. Abadal, N. Barniol, and F. Pérez-Murano, A compact and low-power CMOS circuit for fully integrated NEMS resonators, IEEE Trans. Circuits Syst. I **54**, 377 (2007).

[9] M. S. Hanay, S. I. Kelber, C. D. O'Connell, P. Mulvaney, J. E. Sader, and M. L. Roukes, Inertial imaging with nanomechanical systems, Nat. Nanotechnol. **10**, 339 (2015).

[10] J. Chaste, A. Eichler, J. Moser, G. Ceballos, R. Rurali, and A. Bachtold, A nanomechanical mass sensor with yoctogram resolution, Nat. Nanotechnol. **7**, 301 (2012).

[11] R. W. Peterson, T. P. Purdy, N. S. Kampel, R. W. Andrews, P. L. Yu, K. W. Lehnert, and C. A. Regal, Laser Cooling of a Micromechanical Membrane to the Quantum Backaction Limit, Phys. Rev. Lett. **116**, 063601 (2016).

[12] J. Suh, A. J. Weinstein, C. U. Lei, E. E. Wollman, S. K. Steinke, P. Meystre, A. A. Clerk, and K. C. Schwab, Mechanically detecting and avoiding the quantum fluctuations of a microwave field, Science **344**, 1262 (2014).

[13] T. A. Palomaki, J. W. Harlow, J. D. Teufel, R. W. Simmonds, and K. W. Lehnert, Coherent state transfer between itinerant microwave fields and a mechanical oscillator, Nature (London) **495**, 210 (2013).

[14] A. D. O'Connell, M. Hofheinz, M. Ansmann, R. C. Bialczak, M. Lenander, E. Lucero, M. Neeley, D. Sank, H. Wang, M. Weides, J. Wenner, J. M. Martinis, and A. N. Cleland, Quantum ground state and single-phonon control of a mechanical resonator, Nature (London) **464**, 697 (2010).

[15] D. Rugar and P. Grütter, Mechanical Parametric Amplification and Thermomechanical Noise Squeezing, Phys. Rev. Lett. **67**, 699 (1991).

[16] A. Eichler, J. Chaste, J. Moser, and A. Bachtold, Parametric amplification and self-oscillation in a nanotube mechanical resonator, Nano Lett. **11**, 2699 (2011).

[17] J. Suh, M. D. Lahaye, P. M. Echternach, K. C. Schwab, and M. L. Roukes, Parametric amplification and back-action noise squeezing by a qubit-coupled nanoresonator, Nano Lett. **10**, 3990 (2010).

[18] E. E. Wollman, C. U. Lei, A. J. Weinstein, J. Suh, A. Kronwald, F. Marquardt, A. A. Clerk, and K. C. Schwab, Quantum squeezing of motion in a mechanical resonator, Science **349**, 952 (2015).

[19] J.-M. Pirkkalainen, E. Damskägg, M. Brandt, F. Massel, and M. A. Sillanpää, Squeezing of Quantum Noise of Motion in a Micromechanical Resonator, Phys. Rev. Lett. **115**, 243601 (2015).

[20] A. S. Zibrov, M. D. Lukin, and M. O. Scully, Nondegenerate Parametric Self-Oscillation via Multiwave Mixing in Coherent Atomic Media, Phys. Rev. Lett. **83**, 4049 (1999).

[21] D. Leenov, Gain and noise figure of a variable-capacitance up-converter, Bell Labs Tech. J. **37**, 989 (1958).

[22] A. Olkhovets, D. Carr, J. Parpia, and H. G. Craighead, Nondegenerate nanomechanical parametric amplifier, in *Proceedings of the 14th IEEE International Conference on Micro Electro Mechanical Systems, 2001* (IEEE, New York, 2001), p. 298.

[23] R. Baskaran and K. Turner, "Mechanical domain nondegenerate parametric resonance in torsional mode micro-electro-mechanical oscillator," in *Proceedings of TRANSDUCERS 2003, 12th International Conference on Solid-State Sensors, Actuators and Microsystems* (IEEE, New York, 2003), pp. 863–866.

[24] T. Faust, J. Rieger, M. J. Seitner, J. P. Kotthaus, and E. M. Weig, Coherent control of a classical nanomechanical two-level system, Nat. Phys. **9**, 485 (2013).

[25] I. Mahboob, K. Nishiguchi, H. Okamoto, and H. Yamaguchi, Phonon-cavity electromechanics, Nat. Phys. **8**, 387 (2012).

[26] R. De Alba, F. Massel, I. R. Storch, T. S. Abhilash, A. Hui, P. L. McEuen, H. G. Craighead, and J. M. Parpia, Tunable phonon cavity coupling in graphene membranes, Nat. Nanotechnol. **11**, 741 (2016).

[27] H. Okamoto, A. Gourgout, C. Chang, K. Onomitsu, I. Mahboob, E. Y. Chang, and H. Yamaguchi, Coherent phonon manipulation in coupled mechanical resonators, Nat. Phys. **9**, 480 (2013).

[28] J. P. Mathew, R. N. Patel, A. Borah, R. Vijay, and M. M. Deshmukh, Dynamic strong coupling and parametric amplification in mechanical modes of graphene, Nat. Nanotechnol. **11**, 747 (2016).

[29] A. Gaidarzhy, J. Dorignac, G. Zolfagharkhani, M. Imboden, and P. Mohanty, Energy measurement in nonlinearly

coupled nanomechanical modes, Appl. Phys. Lett. **98**, 264106 (2011).

[30] T. Dunn, J.-S. Wenzler, and P. Mohanty, Anharmonic modal coupling in a bulk micromechanical resonator, Appl. Phys. Lett. **97**, 123109 (2010).

[31] Q. P. Unterreithmeier, E. M. Weig, and J. P. Kotthaus, Universal transduction scheme for nanomechanical systems based on dielectric forces, Nature (London) **458**, 1001 (2009).

[32] I. Mahboob, H. Okamoto, K. Onomitsu, and H. Yamaguchi, Two-Mode Thermal-Noise Squeezing in an Electromechanical Resonator, Phys. Rev. Lett. **113**, 167203 (2014).

[33] H. Yamaguchi and I. Mahboob, Parametric mode mixing in asymmetric doubly clamped beam resonators, New J. Phys. **15**, 015023 (2013).

[34] S. Cho, S. G. Kim, K. Hong, S.-B. Shim, M. Jo, S. U. Cho, and Y. D. Park, Investigation of thermomechanical motion in a nanomechanical resonator based on optical intensity mapping, J. Korean Phys. Soc. **71**, 684 (2017).

[35] D. J. Wilson, C. A. Regal, S. B. Papp, and H. J. Kimble, Cavity Optomechanics with Stoichiometric SiN Films, Phys. Rev. Lett. **103**, 207204 (2009).

[36] S. S. Verbridge, H. G. Craighead, and J. M. Parpia, A megahertz nanomechanical resonator with room temperature quality factor over a million, Appl. Phys. Lett. **92**, 013112 (2008).

[37] A. Bokaian, Natural frequencies of beams under tensile axial loads, J. Sound Vib. **142**, 481 (1990).

[38] S. S. Verbridge, J. M. Parpia, R. B. Reichenbach, L. M. Bellan, and H. G. Craighead, High quality factor resonance at room temperature with nanostrings under high tensile stress, J. Appl. Phys. **99**, 124304 (2006).

[39] See Supplemental Material at http://link.aps.org/supplemental/10.1103/PhysRevApplied.9.064023 for a detailed derivation of the theoretical model and equations for the coupled dynamics. The estimation of amplification gain, cooling by red-detuned sideband parametric pump, and theoretically expected responses of two flexural modes by strong blue-detuned parametric pump are also presented with the experimental results.

[40] M. Poot and H. S. J. van der Zant, Mechanical systems in the quantum regime, Phys. Rep. **511**, 273 (2012).

[41] A. H. Nayfeh and D. T. Mook, *Nonlinear Oscillations* (Wiley-VCH Verlag GmbH, Weinheim, 2007).

[42] A. H. Nayfeh and D. T. Mook, Parametric excitations of linear systems having many degrees of freedom. Acoust. Soc. Am. **62**, 375 (1977).

[43] A. N. Cleland, *Foundations of Nanomechanics* (Springer, New York, 2003).

[44] J. M. Dobrindt, I. Wilson-Rae, and T. J. Kippenberg, Parametric Normal-Mode Splitting in Cavity Optomechanics, Phys. Rev. Lett. **101**, 263602 (2008).

[45] R. Lifshitz and M. C. Cross, Response of parametrically driven nonlinear coupled oscillators with application to micromechanical and nanomechanical resonator arrays, Phys. Rev. B **67**, 134302 (2003).

[46] A. Eichler, J. Moser, J. Chaste, M. Zdrojek, I. Wilson-Rae, and A. Bachtold, Nonlinear damping in mechanical resonators made from carbon nanotubes and graphene, Nat. Nanotechnol. **6**, 339 (2011).

[47] E. Buks and B. Yurke, Mass detection with a nonlinear nanomechanical resonator, Phys. Rev. E **74**, 046619 (2006).

[48] H. B. Chan and C. Stambaugh, Fluctuation-enhanced frequency mixing in a nonlinear micromechanical oscillator, Phys. Rev. B **73**, 224301 (2006).

[49] D. N. Guerra, A. R. Bulsara, W. L. Ditto, S. Sinha, K. Murali, and P. Mohanty, A noise-assisted reprogrammable nanomechanical logic gate, Nano Lett. **10**, 1168 (2010).

[50] J. S. Wenzler, T. Dunn, T. Toffoli, and P. Mohanty, A nanomechanical Fredkin gate, Nano Lett. **14**, 89 (2014).